High-Temperature Synthesis of Two New Aluminophosphates, $NaRb_2Al_2(PO_4)_3$ and $NaCs_2Al(PO_4)_2$, in Molten Alkali Metal Chloride Media

Qun Huang and Shiou-Jyh Hwu*

Department of Chemistry and Materials Science & Engineering Program, Clemson University, Clemson, South Carolina 29634-0973

Received November 17, 2000. Revised Manuscript Received February 27, 2001

Two new aluminophosphate (AlPO) phases have been isolated via conventional solid-state reactions employing molten alkali metal chloride salts. Their structures have been determined by single-crystal X-ray diffraction methods. Crystal data: $NaRb_2Al_2(PO_4)_3$ **1**, $P2_1/c$ (no. 14), $a = 4.849(2)$ Å, $b = 8.216(2)$ Å, $c = 28.317(3)$ Å, $\beta = 90.52(2)°$, and $Z = 4$; $NaCs_2Al(PO_4)_2$ **2**, $P2_1/c$ (no. 14), $a = 10.992(2)$ Å, $b = 9.192(2)$ Å, $c = 18.998(2)$ Å, $\beta = 90.35(1)°$, and $Z = 8$. **1** adopts a new structure type that contains puckered slabs of vertex-sharing AlO_4, AlO_5, and PO_4 polyhedral units. The slab structure is made of interlinked $[Al_2P_3O_{16}]$ structural units resulting in a new $4 \times 6 \times 8$ network of alternating Al^{3+} and P^{5+} cations. It exhibits a unique Al_3P_2 trigonal bipyramidal chain of fused butterfly-like Al_2P_3 units. **2** represents a new three-dimensional compound of the $Al(PO_4)_2^{3-}$ type that consists of alternating, vertex-sharing AlO_4 and PO_4 units. The framework possesses a helical structure embracing around the mixed Na^+ and Cs^+ cations into a 10-ring channel. **1** and **2**, although containing similar polyhedral units as those isolated under hydrothermal conditions, adopt different types of network connectivity, in part, due to the incorporation of alkali metal cations as opposed to organic templates. The new discoveries give insights into the synthesis of thermally stable open-framework AlPOs via high-temperature, solid-state reactions.

Introduction

Open-framework aluminophosphate (AlPO) phases have been extensively studied for their structural diversity as well as potential applications in catalysis and separation. Low-temperature hydrothermal (or solvothermal) conditions have been employed, in part, to avoid structural condensation and to accommodate the relatively low thermal stability of the employed solvents. Via high-temperature, molten-salt synthesis, we have recently isolated a new AlPO phase, $Cs_2Al_2P_2O_9$, which exhibits the rarely seen Al−O−Al linkage.[1] Continued investigations into the crystal growth in molten salt media have resulted in several new AlPO phases. In this report, we will describe the synthesis and structures of two new AlPO phases, $NaRb_2Al_2(PO_4)_3$ **1** and $NaCs_2Al(PO_4)_2$ **2**, adopting totally new structures compared to those isolated under conventional hydrothermal conditions.

Through low-temperature synthesis, a large collection of organically templated AlPO compounds has been discovered. Their structures adopt frameworks ranging from a one-dimensional (1D) chain to a two-dimensional (2D) layer and a three-dimensional (3D) network with almost every given Al/P ratio. When the polyhedral linkage is modified with discrete molecules, such as organic templates, a large variation on the overall framework can result. Compounds having the $[Al_3(PO_4)_4]^{3-}$ stoichiometry, a frequently encountered framework composition, adopt 2D layered structures with 4×6, 4×8, $4 \times 6 \times 8$, and $4 \times 6 \times 12$ networks,[2] and 3D lattices.[3] As to the $[Al_2(PO_4)_3]^{3-}$ and $[Al(PO_4)_2]^{3-}$ types, a large collection of structurally diversified compounds has also been reported. For those having the $[Al_2(PO_4)_3]^{3-}$ composition,[4] there are structures made of layers, such as $Ca_4Mg(H_2O)_{12}[Al_4(OH)_4(PO_4)_6]$,[4a] $(2\text{-}BuNH_3)[HAl_2(PO_4)_3]$,[4b] $(pyH)[H_2Al_2(PO_4)_3]$,[4b] $[C_5H_9NH_3]_2[HAl_2(PO_4)_3]$,[4c] and $[C_6NH_8][Al_2P_3O_{10}(OH)_2]$,[4d] and networks, such as $[Al_2P_3O_{12}](C_4N_3H_{16})$.[5] For $[Al(PO_4)_2]^{3-}$, there are structures composed of chains,[6] such as $Na_4[Al(PO_4)_2(OH)]$,[6a] $Na_3[Al(OH)(HPO_4)(PO_4)]$,[6b] $[Et_3NH][H_2Al(PO_4)_2]$,[6c] and $[C_{10}N_2H_9]$ $[Al(PO_4)(PO_2(OH)_2)]$,[6d] layers,[7] such as

(1) Huang, Q.; Hwu, S.-J. *Chem. Commun.* **1999**, 2343.

(2) (a) Morgan, K.; Gainsford, G.; Milestone, N. *J. Chem. Soc., Chem. Commun.* **1995**, 425. (b) Williams, I. D.; Gao, Q.; Chen, J.; Ngai, L.-Y.; Lin, Z.; Xu, R. *J. Chem. Soc., Chem. Commun.* **1996**, 1781. (c) Yu, J.; Li, J.; Sugiyama, K.; Togashi, N.; Terasaki, O.; Hiraga, K.; Zhou, B.; Qiu, S.; Xu, R. *Chem. Mater.* **1999**, *11*, 1727. (d) Vidal, L.; Marichal, C.; Gramlich, V.; Patarin, J.; Gabelica, Z. *Chem. Mater.* **1999**, *11*, 2728. (e) Jones, R. H.; Thomas, J. M.; Cheetham, A. K.; Powell, A. V. *J. Chem. Soc., Chem. Commun.* **1991**, 1266. (f) Thomas, J. M.; Jones, R. H.; Xu, R.; Chen, J.; Chippindale, A. M.; Natarajan, S.; Cheetham, A. K. *J. Chem. Soc., Chem. Commun.* **1992**, 929.

(3) Xu, Y.-H.; Zhang, B.-G.; Chen, X.-F.; Liu, S.-H.; Duan, C.-Y.; You, X.-Z. *J. Solid State Chem.* **1999**, *145*, 220.

(4) (a) Moore, P. B.; Araki, T. *American Mineralogist* **1974**, *59*, 843. (b) Chippindale, A. M.; Powell, A. V.; Bull, L. M.; Jones, R. H.; Cheetham, A. K.; Thomas, J. M.; Xu, R. *J. Solid State Chem.* **1992**, *96*, 199. (c) Oliver, S.; Kuperman, A.; Lough, A.; Ozin, G. A. *Chem. Mater.* **1996**, *8*, 2391. (d) Yu, J.; Sugiyama, K.; Hiraga, K.; Togashi, N.; Terasaki, O.; Tanaka, Y.; Nakata, S.; Qiu, S.; Xu, R. *Chem. Mater.* **1998**, *10*, 3636.

(5) Wei, B.; Zhu, G.; Yu, J.; Qiu, S.; Xiao, F.; Terasaki, O. *Chem. Mater.* **1999**, *11*, 3417.

10.1021/cm000915c CCC: $20.00
Published on Web 04/21/2001

$[N_2C_3H_5][H_2Al(PO_4)_2]\cdot 2H_2O$,[7a] $[NH_4]_3[Co(NH_3)_6]_3[Al_2(PO_4)_4]_2$,[7b] and $(C_5NH_6)[Al(HPO_4)_2(H_2O)_2]$,[7a] and frameworks,[8] such as $KAl(HPO_4)_2(H_2O)$. The title compounds were synthesized in the absence of discrete organic molecules and hydrogen bonds. Their structural comparisons with the existing network structures will be discussed.

Experimental Section

Synthesis. All chemicals were used as received: Na_2O_2 (Aldrich, 97% purity), Na_2O (Alfa, 86%), RbCl (Alfa, 99.95%), CsCl (Strem, 99.9%), CuO (Strem, 99.999%), $Cu(OH)_2$ (Alfa, 94%), P_2O_5 (Aldrich, 98+%), $(NH_4)_2HPO_4$ (Aldrich, 99%), $Al(OH)_3$ (Cerac, 99.9%), Al powder (Alfa, 99.8%), and NaOH (EMS, 97%).

*$NaRb_2Al_2(PO_4)_3$ (**1**).* High-temperature, solid-state reaction of Na_2O, Rb_2O, Al_2O_3, and P_2O_5 in a mole ratio of 1:2:2:3 along with the eutectic flux NaCl/RbCl (mp = 540 °C) for 1 day at 600 °C give greater than 90% yield of **1**. These optimized synthetic conditions were determined empirically after the observation of **1** in the reaction of Na_2O_2, Al powder, CuO, and P_2O_5 in a mole ratio of 1:1:1:1 along with the halide flux RbCl (mp = 715 °C). The flux-to-charge ratio was 3:1 by weight. The mixture was ground and loaded in a nitrogen filled drybox. The sample was sealed in a quartz ampule under vacuum and then heated to 800 °C according to the procedures reported elsewhere.[1] Colorless transparent needle crystals of **1** (ca. 50% yield) as well as some unidentified polycrystalline phases were retrieved from the flux by washing the products with deionized water using suction filtration.

*$NaCs_2Al(PO_4)_2$ (**2**).* In an open quartz container, solid-state synthesis of NaOH, $CsOH\cdot H_2O$, $Al(OH)_3$ (or Al_2O_3), and $(NH_4)_2HPO_4$ in a mole ratio of 1:2:1(or 0.5):2 for 1 day at 650 °C followed by slow cooling to room temperature gives a stoichiometric yield of **2**. The optimized synthetic conditions of **2** were acquired empirically also after the structure determination. The crystals of **2** were obtained originally from the reaction of Na_2O, $Al(OH)_3$, CuO, P_2O_5, and CsCl (mp = 645 °C) in a mole ratio of 2:1:3:1.5:3. The mixture was ground and loaded into a copper tubing (1.65-in. i.d.)[9] in a nitrogen blanketed drybox. The reaction mixture was heated to 650 °C at 0.5 °C/min and isothermed for 72 h; the reaction was then slowly cooled to ca. 200 °C at 0.15 °C/min and followed by furnace cooling. Washing the products with deionized water using suction filtration retrieved colorless chunk crystals of **2** (ca. 20% yield) and some unidentified polycrystalline phases.

The products of high-yield synthesis were examined by powder X-ray diffraction methods. The refined cell constants[10] of the as-prepared materials **1** and **2** are consistent with the ones obtained from the single-crystal data.

Table 1. Crystallographic Data for $NaRb_2Al_2(PO_4)_3$ (1) and $NaCs_2Al(PO_4)_2$ (2)

compd	**1**	**2**
chem formula	$NaRb_2Al_2P_3O_{12}$	$NaCs_2AlP_2O_8$
fw	532.8	505.7
space group	$P2_1/c$	$P2_1/c$
a, Å	4.849(2)	10.992(2)
b, Å	8.216(2)	9.192(2)
c, Å	28.317(3)	18.998(2)
β, deg	90.52(2)	90.35(1)
V, Å^3	1128.1(6)	1919.7(5)
Z	4	8
T, °C	23	23
λ, Å	0.71073	0.71073
ρ_{calcd}, g/cm^3	3.137	3.500
μ(Mo Kα), mm^{-1}	9.358	8.078
$R(F_o)$,[a] %	2.38	2.87
R_w,[b] %	2.37	3.92

[a] $R = \Sigma||F_o| - |F_c||/\Sigma|F_o|$. [b] $R_w = [\Sigma w[|F_o| - |F_c|]^2/\Sigma w|F_o|^2]^{1/2}$; $w = 1/[\sigma^2(F) + aF^2]$ ($a = 0.0002$ for **1** and 0.0005 for **2**).

Single-Crystal X-ray Diffraction. Crystals of **1** (0.36 × 0.05 × 0.05 mm) and **2** (0.31 × 0.22 × 0.10 mm) were selected and mounted on glass fibers for X-ray single-crystal diffraction studies. The crystallographic data of **1** and **2** are given in Table 1. The diffraction data were collected on the Siemens *R*3*m*/*v* (Mo Kα, $\lambda = 0.71073$ Å) equipped with a graphite monochromator. Unit cell constants were obtained based on least-squares fits of up to 50 reflections. No detectable decay was observed, judging from the intensities of three standard reflections measured every 97 reflections. Lorentz-polarization and empirical absorption corrections[11] (ψ scans) were applied to the data.

The structures were solved by direct methods with SHELXS-86[12] and refined on $|F|$ with SHELXTL-Plus[13] by least-squares, full-matrix techniques.[14] The positions of the alkali metal (Na, Rb, Cs), Al, P, and some oxygen atoms were obtained directly from the Fourier synthesis map, and those of the remaining atoms were determined from the difference Fourier maps. The atomic coordinates and equivalent thermal parameters are listed in Table 2, and the selected bond distances and angles for **1** and **2** are in Tables 3 and 4, respectively. It is noted that large values of the temperature factors of the Rb^+ and Cs^+ cations in compounds **1** and **2**, respectively, are likely due to the big size of cavities in which these cations reside.

Thermogravimetric Analysis. Thermogravimetric analyses (TGA) of as-prepared powder show no weight change up to 1000 °C. Powder X-ray diffraction patterns reveal that the thermally treated products retain the original structures, suggesting the title compounds are stable up to 1000 °C.

Results and Discussion

Single crystals of the new AlPO phases that otherwise would only be made in a polycrystalline form were isolated in molten alkali metal chloride media. This approach is rather unique compared to the conventional hydrothermal synthesis. The products isolated under hydrothermal conditions are often meta-stable, in part, attributed to the thermal instability of incorporated solvent molecules. In contrast, the new family of transi-

(6) (a) Attfield, M. P.; Morris, R. E.; Burshtein, I.; Campana, C. F.; Cheetham, A. K. *J. Solid State Chem.* **1995**, *118*, 412. (b) Lii, K.-H.; Wang, S.-L. *J. Solid State Chem.* **1997**, *128*, 21. (c) Jones, R. H.; Thomas, J. M.; Xu, R.; Huo, Q. S.; Xu, Y.; Cheetham, A. K.; Bieber, D. *J. Chem. Soc., Chem. Commun.* **1990**, 1170. (d) Chippindale, A. M.; Turner, C. *J. Solid State Chem.* **1997**, *128*, 318.

(7) (a) Leech, M. A.; Cowley, A. R.; Prout, K.; Chippindale, A. M. *Chem. Mater.* **1998**, *10*, 451. (b) Morgan, K. R.; Gainsford, G. J.; Milestone, N. B. *Chem. Commun.* **1997**, 61.

(8) Dick, S.; Gossner, U.; Weiss, A.; Robl, C.; Grossmann, G.; Ohms, G.; Müller, M. *J. Solid State Chem.* **1997**, *132*, 47.

(9) The copper tubing was cleaned before and immediately after the first welding by washing with nitric acid and then rinsing with deionized water, followed by drying in an oven. Prior to loading a reaction, one end of the copper tubing was crimped and then welded with a methane torch in air. After the reaction was loaded, the second end of the tubing was then welded outside the drybox. During the second welding, the bottom half of the tubing was immersed in water to keep the reactants from being exposed to the heat. The reaction container was jacketed in quartz tubing (3.2-in. i.d.), which was then sealed off under vacuum.

(10) Powder X-ray diffraction patterns of as-prepared materials were collected by Scintag XDS 2000 (Cu radiation). Cell constants of **1** ($a = 4.850(1)$ Å, $b = 8.216(1)$ Å, $c = 28.308(2)$ Å, $\beta = 90.55(2)°$, $V = 1128.1(4)$ Å^3) and **2** ($a = 10.986(3)$ Å, $b = 9.186(2)$ Å, $c = 18.997(4)$ Å, $\beta = 90.34(2)°$, $V = 1917.0(9)$ Å^3) were acquired by the least−squares refinement of 20 and 17 reflections, respectively. Silicon (NIST) was employed as an internal standard.

(11) North, A. C. T.; Phillips, D. C.; Mathews, F. S. *Acta Crystallogr.* **1968**, *A24*, 351.

(12) Sheldrick, G. M. In *Crystallographic Computing 3*; Sheldrick, G. M., Kruger, C., Goddard, R., Eds.; Oxford University Press: London, 1985; pp 175−189.

(13) Sheldrick, G. M. *SHELXTL-PLUS, Version 4.2.1 Structure Determination Software Programs*; Siemens Analytical X-ray Instruments Inc.: Madison, WI, 1990.

(14) Busing, W. R.; Martin, K. O.; Levy, H. A. *ORFLS*; Report ORNL-TM-305; Oak Ridge National Laboratory: Oak Ridge, TN, 1962.

Table 2. Atomic Coordinates ($\times 10^4$) and Equivalent Isotropic Displacement Coefficients U_{eq} ($\times 10^3$ Å^2) for $NaRb_2Al_2(PO_4)_3$ (1) and $NaCs_2Al(PO_4)_2$ (2)

atom	*x*	*y*	*z*	U_{eq}[a]
		$NaRb_2Al_2(PO_4)_3$ (**1**)		
Rb(1)	2614(1)	4808(1)	1710(1)	19(1)
Rb(2)	2737(1)	1437(1)	478(1)	21(1)
P(1)	2254(2)	2837(1)	2910(1)	7(1)
P(2)	−3021(2)	1926(1)	4517(1)	9(1)
P(3)	2432(2)	6610(1)	3568(1)	8(1)
Al(1)	7322(2)	5293(1)	2924(1)	8(1)
Al(2)	1878(2)	3148(1)	3956(1)	8(1)
Na(1)	−2203(3)	4478(2)	473(1)	15(1)
O(1)	−740(5)	3422(3)	2923(1)	13(1)
O(2)	2456(5)	1249(3)	2638(1)	10(1)
O(3)	3059(6)	2376(3)	3425(1)	12(1)
O(4)	4191(5)	4106(3)	2717(1)	10(1)
O(5)	−1481(5)	2532(4)	4068(1)	17(1)
O(6)	−6138(5)	2277(3)	4405(1)	12(1)
O(7)	2332(6)	8222(3)	3813(1)	14(1)
O(8)	5361(5)	6287(3)	3380(1)	15(1)
O(9)	315(5)	6458(3)	3175(1)	15(1)
O(10)	1915(6)	5253(3)	3950(1)	16(1)
O(11)	2658(6)	5119(3)	424(1)	18(1)
O(12)	2203(6)	−2105(3)	55(1)	17(1)
		$NaCs_2Al(PO_4)_2$ (**2**)		
Cs(1)	6820(1)	333(1)	1328(1)	26(1)
Cs(2)	8150(1)	383(1)	3543(1)	29(1)
Cs(3)	4073(1)	30(1)	3961(1)	23(1)
Cs(4)	850(1)	−30(1)	1183(1)	29(1)
P(1)	3973(1)	−1734(1)	2177(1)	13(1)
P(2)	3380(1)	2111(1)	477(1)	14(1)
P(3)	8784(1)	3129(1)	384(1)	14(1)
P(4)	8537(1)	7285(1)	2011(1)	13(1)
Al(1)	3825(1)	1738(1)	2106(1)	12(1)
Al(2)	8804(1)	6613(1)	410(1)	12(1)
Na(1)	909(2)	−1482(3)	2909(1)	36(1)
Na(2)	6017(2)	1679(2)	−393(1)	23(1)
O(1)	4213(4)	−74(4)	2138(2)	35(1)
O(2)	2691(3)	−2012(5)	2402(2)	37(1)
O(3)	4304(4)	−2437(4)	1495(2)	33(1)
O(4)	5161(3)	2735(4)	2221(2)	25(1)
O(5)	3223(3)	2228(4)	1290(2)	24(1)
O(6)	2287(4)	3047(6)	206(2)	52(2)
O(7)	3197(6)	591(4)	247(2)	54(2)
O(8)	4526(4)	2793(6)	255(2)	58(2)
O(9)	8961(4)	4764(4)	556(2)	36(1)
O(10)	221(3)	−2731(4)	168(2)	30(1)
O(11)	9002(4)	2304(4)	1056(2)	37(1)
O(12)	7569(4)	2873(5)	63(2)	45(1)
O(13)	8410(3)	−2561(3)	1192(2)	21(1)
O(14)	9058(5)	−1339(5)	2292(2)	50(2)
O(15)	9230(6)	−4025(6)	2200(2)	64(2)
O(16)	7204(3)	−2824(6)	2250(2)	44(2)

[a] Equivalent isotropic *U* defined as one-third of the trace of the orthogonalized $\mathbf{U}_{ij}$ tensor.

tion-metal-containing-microporous (TMCM) solids reported earlier that was prepared in the molten salt media has demonstrated an enhanced thermal stability up to 650 °C.[15] The present studies are part of the continued efforts on the exploratory synthesis of new TMCM aluminophosphate phases. The new findings suggest that AlPO frameworks with respect to layers and channels (see below) form at high temperatures in the absence of water and organic templates.

During the synthesis of **2**, copper tubing was employed as a reaction vessel to contain the water vapor pressure generated from the thermal decomposition of $Al(OH)_3$. The use of aluminum hydroxide as a starting material is, like aluminum powder, to produce reactive aluminum oxide in situ to promote the AlPO formation.

(15) (a) Huang, Q.; Ulutagay, M.; Michener, P. A.; Hwu, S.-J. *J. Am. Chem. Soc.* **1999**, *121*, 10323. (b) Huang, Q.; Hwu, S.-J. *Angew. Chem.*, in press.

Table 3. Selected Bond Lengths (Å) and Angles (deg) for $NaRb_2Al_2(PO_4)_3$ (1)

P(1)−O(1)	1.530(3)	P(3)−O(10)	1.576(3)
P(1)−O(2)	1.519(3)	Al(1)−O(4)	1.894(3)
P(1)−O(3)	1.553(3)	Al(1)−O(8)	1.805(3)
P(1)−O(4)	1.509(3)	Al(1)−O(1)[c]	1.802(3)
P(2)−O(5)	1.561(3)	Al(1)−O(2)[d]	1.779(3)
P(2)−O(6)	1.568(3)	Al(1)−O(9)[c]	1.872(3)
P(2)−O(11)[a]	1.504(3)	Al(2)−O(3)	1.733(3)
P(2)−O(12)[a]	1.501(3)	Al(2)−O(5)	1.738(3)
P(3)−O(7)	1.497(3)	Al(2)−O(10)	1.730(3)
P(3)−O(8)	1.544(3)	Al(2)−O(6)[c]	1.742(3)
P(3)−O(9)	1.513(3)		
O(2)−P(1)−O(4)	111.5(1)	O(9)−P(3)−O(10)	109.6(2)
O(3)−P(1)−O(4)	110.9(1)	O(4)−Al(1)−O(8)	91.6(1)
O(1)−P(1)−O(2)	110.3(2)	O(4)−Al(1)−O(1)[c]	88.6(1)
O(1)−P(1)−O(3)	106.6(2)	O(8)−Al(1)−O(1)[c]	131.8(1)
O(2)−P(1)−O(3)	104.5(1)	O(4)−Al(1)−O(2)[d]	90.3(1)
O(1)−P(1)−O(4)	112.7(2)	O(8)−Al(1)−O(2)[d]	118.5(1)
O(5)−P(2)−O(6)	104.1(1)	O(1)[c]−Al(1)−O(2)[d]	109.8(1)
O(5)−P(2)−O(11)[a]	110.4(2)	O(4)−Al(1)−O(9)[c]	175.8(1)
O(6)−P(2)−O(11)[a]	108.4(2)	O(8)−Al(1)−O(9)[c]	84.8(1)
O(5)−P(2)−O(12)[a]	111.3(2)	O(1)[c]−Al(1)−O(9)[c]	92.0(1)
O(6)−P(2)−O(12)[a]	108.2(2)	O(2)[d]−Al(1)−O(9)[c]	93.5(1)
O(11)[a]−P(2)−O(12)[a]	113.8(2)	O(3)−Al(2)−O(6)[c]	107.4(1)
O(7)−P(3)−O(8)	110.3(2)	O(5)−Al(2)−O(6)[c]	105.0(1)
O(7)−P(3)−O(9)	112.9(2)	O(10)−Al(2)−O(6)[c]	114.3(1)
O(8)−P(3)−O(9)	110.6(1)	O(3)−Al(2)−O(5)	111.7(1)
O(7)−P(3)−O(10)	107.5(1)	O(3)−Al(2)−O(10)	110.8(1)
O(8)−P(3)−O(10)	105.6(2)	O(5)−Al(2)−O(10)	107.6(2)

[a] Symmetry code: $-x, -0.5 + y, 0.5 - z$. [b] Symmetry code: $-x, 0.5 + y, -0.5 - z$. [c] Symmetry code: $1 + x, y, z$. [d] Symmetry code: $1 - x, 0.5 + y, 0.5 - z$.

Table 4. Selected Bond Lengths (Å) and Angles (deg) for $NaCs_2Al(PO_4)_2$ (2)

P(1)−O(1)	1.550(4)	P(4)−O(13)[c]	1.568(3)
P(1)−O(2)	1.497(4)	P(4)−O(14)[c]	1.487(5)
P(1)−O(3)	1.495(4)	P(4)−O(15)[c]	1.468(6)
P(1)−O(4)[a]	1.562(4)	P(4)−O(16)[c]	1.540(4)
P(2)−O(5)	1.560(3)	Al(1)−O(1)	1.721(4)
P(2)−O(6)	1.563(5)	Al(1)−O(4)	1.743(4)
P(2)−O(7)	1.477(4)	Al(1)−O(5)	1.741(3)
P(2)−O(8)	1.471(5)	Al(1)−O(16)[d]	1.719(4)
P(3)−O(9)	1.550(4)	Al(2)−O(9)	1.731(4)
P(3)−O(11)	1.504(4)	Al(2)−O(6)[b]	1.699(5)
P(3)−O(12)	1.483(4)	Al(2)−O(10)[e]	1.735(4)
P(3)−O(10)[b]	1.564(4)	Al(2)−O(13)[c]	1.727(3)
O(1)−P(1)−O(2)	110.1(2)	O(13)[c]−P(4)−O(14)[c]	108.1(2)
O(1)−P(1)−O(3)	109.9(2)	O(13)[c]−P(4)−O(15)[c]	111.1(2)
O(2)−P(1)−O(3)	114.1(2)	O(14)[c]−P(4)−O(15)[c]	114.3(3)
O(1)−P(1)−O(4)[a]	103.9(2)	O(13)[c]−P(4)−O(16)[c]	102.6(2)
O(2)−P(1)−O(4)[a]	108.0(2)	O(14)[c]−P(4)−O(16)[c]	108.4(3)
O(3)−P(1)−O(4)[a]	110.4(2)	O(15)[c]−P(4)−O(16)[c]	111.6(3)
O(5)−P(2)−O(6)	101.4(2)	O(1)−Al(1)−O(4)	107.2(2)
O(5)−P(2)−O(7)	110.0(2)	O(1)−Al(1)−O(5)	112.0(2)
O(6)−P(2)−O(7)	108.7(3)	O(4)−Al(1)−O(5)	107.0(2)
O(5)−P(2)−O(8)	110.8(2)	O(1)−Al(1)−O(16)[d]	111.4(2)
O(6)−P(2)−O(8)	109.2(3)	O(4)−Al(1)−O(16)[d]	110.2(2)
O(7)−P(2)−O(8)	115.7(3)	O(5)−Al(1)−O(16)[d]	109.0(2)
O(9)−P(3)−O(11)	106.9(2)	O(9)−Al(2)−O(6)[b]	111.1(2)
O(9)−P(3)−O(12)	110.7(3)	O(9)−Al(2)−O(10)[e]	107.1(2)
O(11)−P(3)−O(12)	114.0(3)	O(6)[b]−Al(2)−O(10)[e]	112.6(2)
O(9)−P(3)−O(10)[b]	106.3(2)	O(9)−Al(2)−O(13)[c]	108.6(2)
O(11)−P(3)−O(10)[b]	110.1(2)	O(6)[b]−Al(2)−O(13)[c]	109.5(2)
O(12)−P(3)−O(10)[b]	108.6(2)	O(10)[e]−Al(2)−O(13)[c]	107.8(2)

[a] Symmetry code: $1 - x, -0.5 + y, 0.5 - z$. [b] Symmetry code: $1 - x, -y, -z$. [c] Symmetry code: $x, 1 + y, z$. [d] Symmetry code: $1 - x, 0.5 + y, 0.5 - z$. [e] Symmetry code: $1 + x, 1 + y, z$.

Structure of $NaRb_2Al_2(PO_4)_3$ (1). 1 adopts a layered structure, as shown in Figure 1, that consists of slabs of fused $[Al_2P_3O_{16}]$ units through bridging oxygen

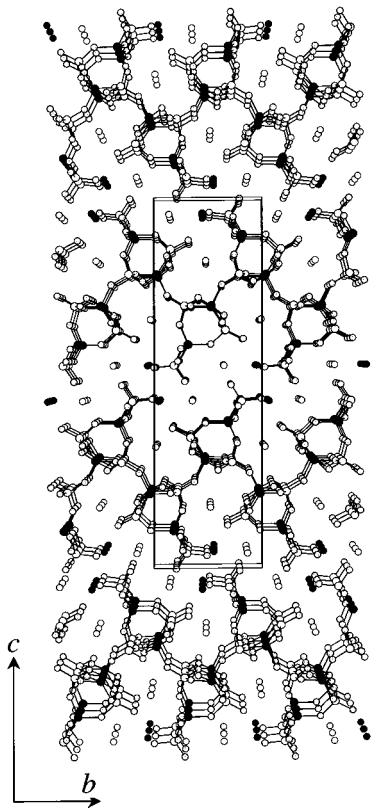

Figure 1. Projected structure of $NaRb_2Al_2(PO_4)_3$ (**1**) viewed along the *a* axis. The $Al_2P_3O_{16}$ units are connected through the bridging oxygen atoms to form puckered AlPO slabs (see text). The Al and P atoms are drawn in large solid and open circles, Na and Rb in small (nonbonded) solid and open circles, and O in (bonded) open circles, respectively. The unit cell is outlined in solid lines.

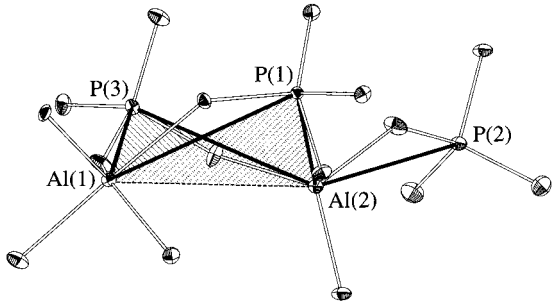

Figure 2. ORTEP drawing of the $Al_2P_3O_{16}$ unit. The thick lines outline the butterfly unit; see text.

atoms. The puckered Al−P−O slabs are stacked along the *c* axis with the Na^+ and Rb^+ cations residing in the interstitial space. The $[Al_2P_3O_{16}]$ structural unit, as shown in Figure 2, consists of a distorted four-membered ring (4MR), which is made of alternating Al^{3+} and P^{5+} cations centered in the 1 × $Al(2)O_4$, 1 × $Al(1)O_5$, and 2 × $P(1,3)O_4$ polyhedra and a "terminal" PO_4 unit. These polyhedra are interconnected via sharing vertex oxygen atoms to form a butterfly unit (as outlined by the shaded 4MR). The terminal PO_4 tetrahedron looking like a tail of the butterfly is connected to the 4MR through the $Al(2)O_4$ tetrahedron. All the Al−O and P−O bond distances (Table 3) are, otherwise, normal and comparable with those observed in the reported AlPO phases. The parallel Al−P−O slabs are interconnected through the Na^+ and Rb^+ cations with the Na−O and Rb−O bond distances in the ranges 2.271(3)−2.569(3) and 2.873(3)−3.511(3) Å. These values are comparable with 2.40 and 3.07 Å, the sum of the Shannon crystal radii of 6-coordinated Na^+ (1.16 Å) and 11-coordinated Rb^+ (1.83 Å) with that of oxygen (1.24 Å), respectively.[16]

The aluminum atoms are coordinated to four and five oxygen atoms. The tetrahedrally coordinated $Al(2)O_4$ has bond distances, 1.730(3)−1.742(3) Å, and bond angles, 104.9°−114.3°, slightly distorted. The trigonal bipyramidal $Al(1)O_5$ unit also shows a slight distortion having two long axial Al−O bonds, 1.872(3) and 1.894(3) Å, along with three short equatorial Al−O linkages, 1.779(3)−1.805(3) Å. The axial O(4)−Al(1)−O(9) bond angle, 175.8(1)°, is off slightly from 180°. The bond valence sum calculations show the value of 3.10 closely matches an Al^{3+} oxidation state.[17]

Among all the layered structures of the $Al_2(PO_4)_3^{3-}$ type, only three consist of trigonal bipyramidal AlO_5 units and, in turn, share the common structural unit $Al_2P_3O_{16}$. Besides **1**, the other two known phases are $(pyH)[H_2Al_2(PO_4)_3]$ (**3**)[4b] and $[C_6NH_8][Al_2P_3O_{10}(OH)_2]$ (**4**).[4d] For a comparison, the slab structures of **1**, **3**, and **4** are shown in Figure 3. The networks are drawn to show the connectivity of the Al^{3+} and P^{5+} cations with the oxide linkages omitted for clarity. From this figure one can see that each of **1** and **3** contains a 4 × 6 × 8 net, while **4** has a 4 × 6 net. Furthermore, both **3** and **4** have the Al_2P_3 units similarly fused in a head-to-tail orientation while **1** has the stacked units in a head-to-head fashion. The stacked butterfly units give rise to a unique Al_3P_2 trigonal bipyramidal geometry. The bipyramidal units are fused into a linear chain through sharing the head of each butterfly unit, Al(1) of the AlO_5 polyhedron. The resulting 4 MRs in **3** and **4**, however, are interlinked through sharing the corner and edge of the square units, a feature commonly seen in a large collection of AlPO networks.

The slabs are held together, instead of by organic molecules, by the alkali metal cations A^+. There is no observable water insertion in a reasonable time frame presumably because of the strong A−O bonding interactions.

Structure of $NaCs_2Al(PO_4)_2$ (2). 2 exhibits a novel three-dimensional open-framework that consists of 10-ring channels. The overall framework is composed of alternating, vertex-sharing AlO_4 and PO_4 tetrahedral units (Figure 4). Depending upon the polyhedral connection, it gives rise to two different types (**I** and **II**) of channel structures (Figure 5) with respect to the different polyhedral arrangements (Figure 6). While **I** and **II** channels are alternating along [100], the channels of the same type are fused and propagated along the [001] direction. In any case, the channels are constructed by embracing the polyhedral network around the multiple alkali metal cations, that is, a total of 2 × Na^+ and 4 × Cs^+ cations occupy each channel as the structure is viewed along the channel direction (Figure 4). Despite the channel framework, there are no ion-exchange properties observed at room temperature in the water medium.

Both channels exhibit nearly identical 10-ring windows (Figure 5). The detailed structural analysis,

(16) Shannon, R. D. *Acta Crystallogr.* **1976**, *A32*, 751.
(17) Brown, I. D.; Altermatt, D. *Acta Crystallogr.* **1985**, *B41*, 244.

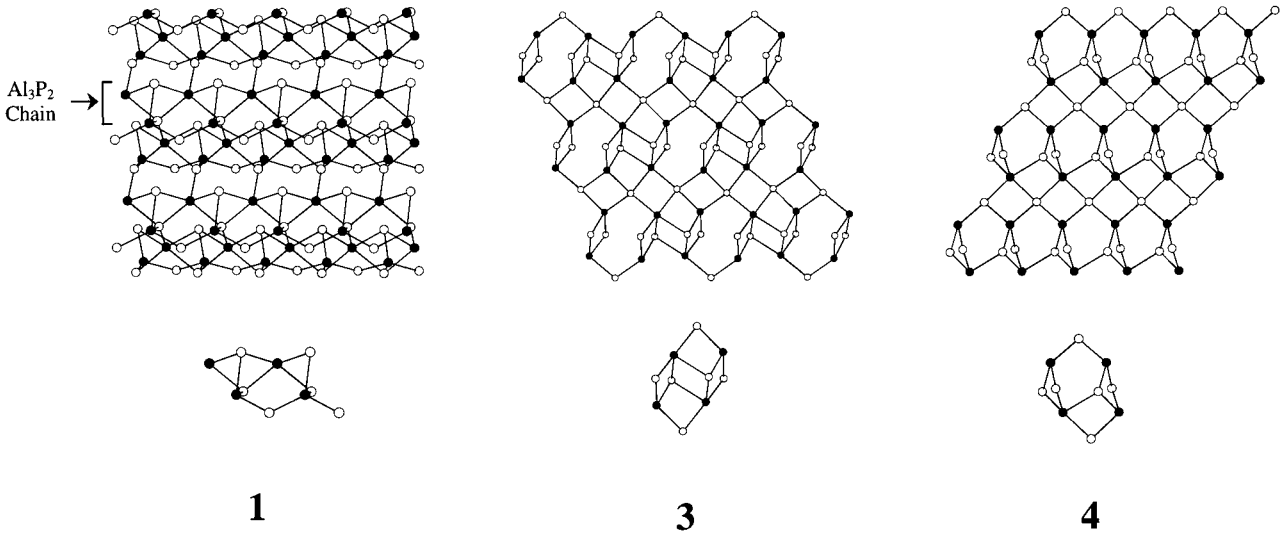

Figure 3. Network structures of $NaRb_2Al_2(PO_4)_3$ (**1**), (pyH)$[H_2Al_2(PO_4)_3]$ (**3**), and $[C_6NH_8][Al_2P_3O_{10}(OH)_2]$ (**4**). Only the Al^{3+} (solid circle) and P^{5+} (open circle) cations are shown for clarity. A double Al_2P_3 unit is drawn for each of the network structures to assist in viewing the network connectivity. The fused Al_2P_3 units result in a unique trigonal bipyramidal Al_3P_2 chain in **1**; see text.

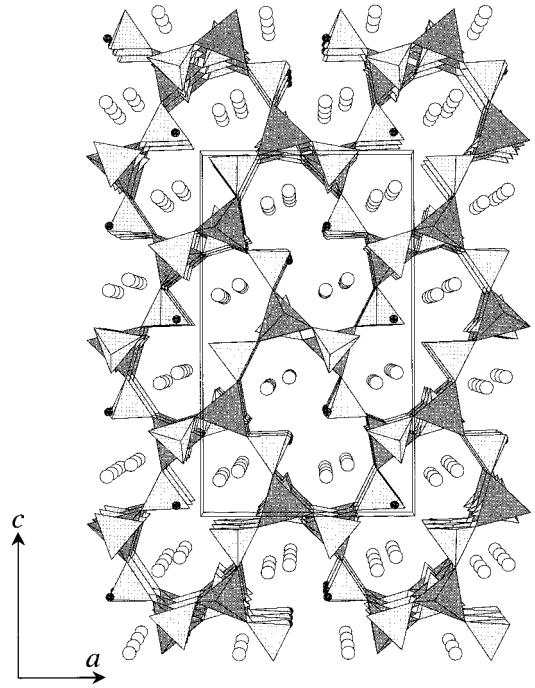

Figure 4. Projected view of $NaCs_2Al(PO_4)_2$ (**2**) along the 10-ring channels. The AlO_4 and PO_4 tetrahedra are shown in dark and light polyhedral drawings, respectively. The Na^+ (solid small circles) and Cs^+ (large open circles) cations reside in the channels; see text.

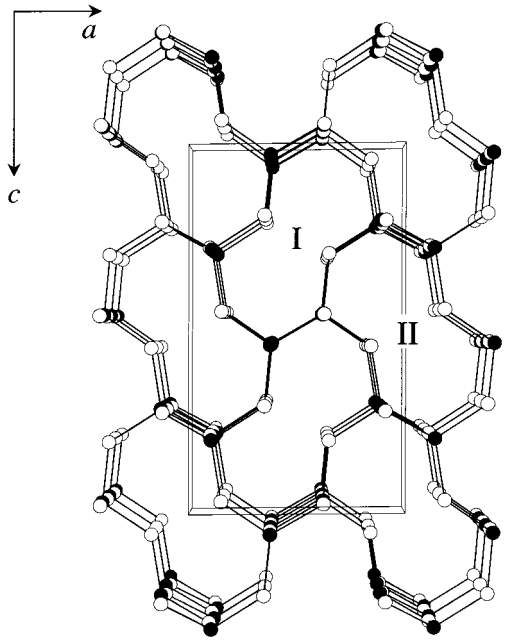

Figure 5. Network structure viewed along two types of channels, **I** and **II**. For the simplicity, only the Al^{3+} (solid circles) and P^{5+} cations (open circles) are drawn. Each channel exhibits a 10-ring window; see text.

however, reveals the difference in network construction (Figure 6). Channel **I** (left, Figure 6) is made of a helical chain of alternating Al_2P_2 4-MRs and AlP_3 T-shape units. Channel **II** (right, Figure 6) is made of fused 12-rings of alternating Al^{3+} and P^{5+} cations. Each 12-ring adopts a puckered configuration, and two of the opposite vertex phosphorus atoms (unshared open circles) are shared with the T-shape units in channel **I**. These P atoms reside in the common corners of 1 × **I** and 2 × **II** channels (Figure 5) and alternate with Al atoms along the channel direction. The 4-MRs mentioned above are shared by the fused channels of type **I**. From the projected view, it also exhibits an alternating array of Al and P atoms in the common corners shared by 2 × **I** and 1 × **II**. This composite structure shows once again the versatility of the aluminophosphate framework.

Each PO_4 unit shares two of its four coordinated oxygen atoms while the AlO_4 unit shares three in an alternating Al^{3+}/P^{5+} network. The PO_4 tetrahedra are slightly distorted having the typical $P-O^b$ (O^b: bridging oxygen) and $P-O^t$ (O^t: terminal oxygen) bond distances on the averages of 1.557(4) and 1.485(4) Å, respectively, and the O−P−O bond angles, ranging from 101.4(2)° to 114.3(3)°; see Table 4. The AlO_4 tetrahedra have the Al−O bond lengths, ranging from 1.699(5) to 1.743(4) Å, and O−Al−O bond angles, from 107.0(2)° to 112.6(2)°, comparable with the reported values.

The Na^+ cation is bonded to four oxygen atoms in a distorted tetrahedral geometry, judging from the widely distributed bond distances, 2.202(5) to 2.345(5) Å, and

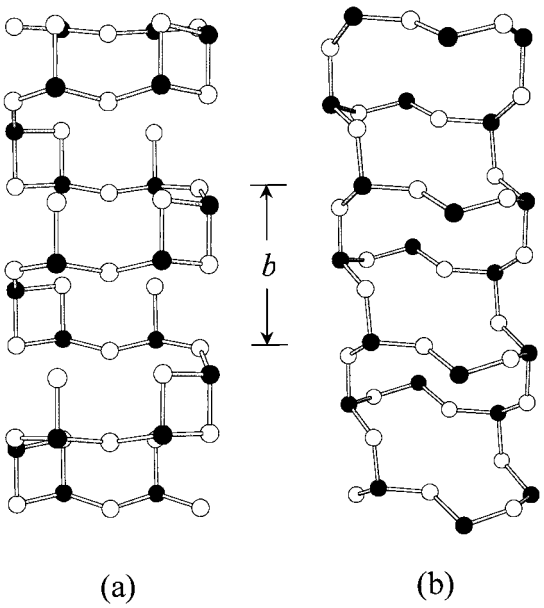

Figure 6. Vertical views of the channels **I** and **II** showing (a) a helical chain of alternating Al_2P_2 4-MRs and AlP_3 T-shape units and (b) a chain of fused 12-rings. The shading codes are the same as those in Figure 5.

O−Na−O bond angles, 80.9(2)° to 128.0(2)°. However, the bond distances are comparable with 2.37 Å of the sum of Shannon crystal radii of four-coordinated Na^+ (1.13 Å) and oxygen (1.24 Å). Cs^+ cations are bonded to 10 oxygen atoms with the Cs−O bond distances randomly distributed between 2.963(4) and 3.792(4) Å. In any case, the bond valence sum calculations based on the given geometry result in the values of 1.11−1.20 and 0.89−1.04 that are consistent with the Na^+ and Cs^+ oxidation states, respectively.

In summary, two new aluminophosphates synthesized in molten salt media exhibit unique framework structures. Employing molten salt not only promotes the crystal growth of refractory oxides but also facilitates the formation of low-dimensional AlPO phases at high temperatures. It is rather unusual to isolate structures with sizable channels via a high-temperature route. The reaction temperature (650 °C) employed for **2** (having the 10-ring channel structure), in fact, is far beyond the maximum temperature commonly utilized under hydrothermal conditions. The multiple alkali metal cations, as opposed to organic templates, residing in the interstitial space may be responsible for the high thermal stability up to 1000 °C. In any event, the research outcomes on high-temperature molten-salt synthesis indicate that open-framework AlPOs with high thermal stabilities are yet to come.

Acknowledgment. We gratefully acknowledge the National Science Foundation (DMR-0077321, CHE-9808165, and EPS-9977797) and South Carolina Commission on Higher Education (R99-06C) for the financial support of this research.

Supporting Information Available: Tables of detailed crystallographic data for **1** and **2**, anisotropic thermal parameters, entire bond distances and angles, PXRD patterns for **1** and **2**, and structure factors (PDF). This information is available free of charge via the Internet at http://pubs.acs.org.

CM000915C